

# A Functional Mapping for Passively Mode-Locked Semiconductor Lasers

S. V. Gurevich  
 Institute for Theoretical Physics  
 University of Munster  
 Münster, Germany

J. Javaloyes, C. Schelte  
 Departament de Física, (ONL)  
 Universitat de les Illes Balears,  
 E-07122 Palma de Mallorca, Spain.

**Abstract**—We present a modern approach for the analysis of passively mode-locked semiconductor lasers that allows for efficient parameter sweeps and time jitter analysis. It permits accessing the ultra-low repetition rate regime where pulses become localized states. The analysis including slow (e.g. thermal) processes or transverse, diffractive dynamics becomes feasible. Our method bridges the divide between the phenomenological, yet highly efficient, pulse iterative model that is the Haus master equation, and the more involved first principle descriptions relying on time delayed equations. Reductions of the simulation times and of the memory footprint up to two orders of magnitudes are demonstrated.

**Index Terms**—Semiconductor laser, Vertical Cavity Surface Emitting Lasers

## I. INTRODUCTION

Generation of low repetition rate picosecond pulses is of paramount importance for a number of applications [1], [2]. Passive Mode-locking (PML) of semiconductor lasers is a most promising method, although it still represents an experimental and a theoretical challenge, see [3] for a recent review. The Haus master equation [4] is an efficient and widely used approach to study PML. It consists in restricting the analysis of the field to a small temporal interval around the pulse. Yet this method, when applied to a particular design, provides only qualitative predictions due to the many simplifying hypothesis involved. How to derive *the* Haus equation, for a specific laser design, is also an open question. On the other hand, first principle modeling allows representing the full dynamics of both unidirectional and bidirectional cavities as either Delay Differential Equations (DDEs) [5] or Delay Algebraic Equations (DAEs) [6], respectively. Such models have been applied successfully to the study of PML with saturable absorber (SA), and were extended to describe photonic crystals [7], external optical feedback [8], coherent optical injection [9], nonlocal imaging conditions [10] and localized structures (LSs) [11].

## II. RESULTS

We illustrate the idea of the functional mapping (FM) [12] using the DDE model of [5] that considers unidirectional propagation in a ring laser. The equations for the field amplitude  $A$ , the gain  $G$  and the absorption  $Q$  read

$$\frac{\dot{A}}{\gamma} = -A + Y(t - \tau), \quad (1)$$

$$\dot{G} = \Gamma(G_0 - G) - e^{-Q} (e^G - 1) |A|^2, \quad (2)$$

$$\dot{Q} = Q_0 - Q - s(1 - e^{-Q}) |A|^2, \quad (3)$$

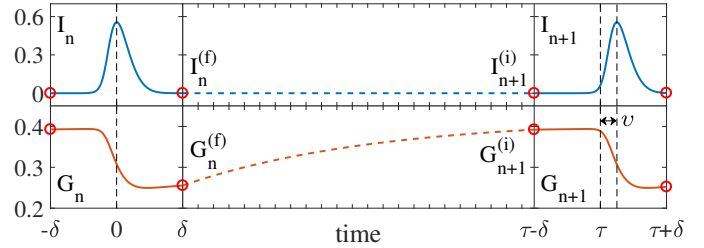


Figure 1. Temporal profile of the intensity  $I_n = |A_n|^2$  and of the gain  $G_n$  at the  $n$ -th and  $n + 1$ -th round-trips. After the emission of the pulse  $I_n$  and the ensuing gain depletion, the so-called fast stage (solid lines), the gain recovers until the next round-trip while the field is vanishing (dashed lines). Knowing the final value of  $G_n^{(f)}$  in the interval  $z \in [-\delta, \delta]$ , one can deduce the initial gain value at the next round-trip  $G_{n+1}^{(i)}$ . The central panel is not up to scale and can be several orders of magnitude larger than the outer panels.

with

$$Y(t) = \exp \left[ \frac{1 - i\alpha}{2} G(t) - \frac{1 - i\beta}{2} Q(t) \right] A(t), \quad (4)$$

where  $G_0$  is the pumping strength,  $\Gamma = \tau_g^{-1}$  the gain recovery rate,  $Q_0$  the value of the unsaturated losses which determines the modulation depth of the SA and  $s$  the ratio of the saturation energy of the gain and of the SA sections. We define  $\kappa$  as the intensity transmission of the output mirror, i.e., the fraction of the power remaining in the cavity after each round-trip. In Eqs. (1-3) time has been normalized to the SA recovery time that we assume to be  $\tau_q = 20$  ps. The linewidth enhancement factor of the gain and absorber sections are noted  $\alpha$  and  $\beta$ , respectively. In addition,  $\gamma$  is the bandwidth of the spectral filter whose central optical frequency has been taken as the carrier frequency for the field. This spectral filter may (coarsely) represent, e.g., the resonance of a VCSEL [10]. If not otherwise stated  $(\kappa, \alpha, \beta, s) = (0.8, 2, 0.5, 30)$ , and  $Q_0 = 0.3$  which corresponds to modulation of the losses of  $\sim 26\%$ . We also set  $\gamma = 10$  and  $\Gamma = 0.04$ , leading to a gain bandwidth full width at half maximum of 160 GHz and  $\tau_g = 500$  ps.

We wrote Eq. (1) in a form that makes apparent that the forcing field  $Y(t - \tau)$  defined in Eq. (4) is a nonlinear function that is known over a whole interval of duration  $\tau$ . Since  $G$  and  $Q$  are functions of  $A$ ,  $Y$  involves *only* the past values of the field, i.e.,  $Y(t - \tau) = g[A(t - \tau)]$ . Knowing the forcing term  $Y$ , Eq. (1) can be solved for  $A$  over an interval of duration  $\tau$ . Integrating Eqs. (1-4), not over the whole round-trips, but only in a selected time interval in

the pulse vicinity, is at the core of our method. We define the field and carrier profiles at the  $n$ -th round-trip as  $A_n(z)$  and  $(G_n, Q_n)(z)$ . For clarity, we set in Fig. 1 the pulse at the origin of time at the  $n$ -th round-trip. Next, we define a small interval of duration  $2\delta$  and a local time  $z \in [-\delta, \delta]$ . Finally, we impose a condition on the waveform  $A_n$ : it is a pulse of duration  $\tau_p$  asymptotic to  $A = 0$  if  $\delta \gg \tau_p$ . Under these approximations, one can solve Eq. (1) using standard integration techniques, e.g., Runge-Kutta method, at the next round-trip, using the following sequence  $(A_n, G_n, Q_n) \rightarrow Y_n \rightarrow (A_{n+1}, G_{n+1}, Q_{n+1})$ . Doing so corresponds to writing a functional mapping  $A_{n+1} = F(A_n)$ . The remainder of the dynamics during the round-trip of duration  $r = t - 2\delta$ , see central panel in Fig. 1, in which the field is vanishing can be found by solving Eqs. (2,3) analytically in the absence of stimulated emission, the so-called slow stage of PML. As such,  $G_{n+1}^{(i)} = G_{n+1}^{(f)}\chi + G_0(1 - \chi)$  with  $\chi = \exp(-\Gamma r)$  and similarly for  $Q_{n+1}^{(i)}$ . Solving analytically the slow stage allows to fully cancel the stiffness inherent to the multiscale nature of PML which is exceptionally useful in the long delay limit  $\tau \gg \tau_g$ . The speedup of our method is equal to the ratio of the actual integration domain  $2\delta$  and of the full round-trip  $\tau$ , i.e.,  $m = \tau / (2\delta)$ . Taking a domain of duration  $2\delta = 5\tau_p$ , a pulse-width of  $\tau_p = 1$  ps at a repetition rate of  $\tau^{-1} = 1$  GHz, yields a speedup  $m = 200$ , i.e., a 24 hour simulation with, e.g., slow thermal effects or transverse diffraction could potentially be achieved in a few ( $\sim 7$ ) minutes.

We conclude our analysis by showing how the FM can be used for the simulation of broad area MIXSEL system described by the DAE model of [6], [10]. The model for the intra-cavity field  $E$ , gain  $N_1$  and absorption  $N_2$  reads

$$\dot{E} = [(1 - i\alpha_1)N_1 + (1 - i\alpha_2)N_2 - 1 + i\Delta_\perp]E + hY \quad (5)$$

$$\dot{N}_1 = \gamma_1(J_1 - N_1) - N_1|E|^2, \quad (6)$$

$$\dot{N}_2 = \gamma_2(J_2 - N_2) - sN_2|E|^2. \quad (7)$$

while the relation linking the intra-cavity ( $E$ ) and external cavity ( $Y$ ) fields is, after proper normalization,

$$Y(t) = \eta[E(t - \tau) - Y(t - \tau)] \quad (8)$$

with  $\eta$  the external mirror reflectivity, see [10] for more details. For the sake of simplicity, we consider diffraction in a single transverse dimension, making the problem two-dimensional and allowing for easier multi-parameter bifurcation analysis. We concentrate on the spatio-temporal localization regime where the field coalesces into a spatio-temporal dissipative soliton, also called a Light Bullet (LB) [13], [14]. Figure 2 (a) shows a two-dimensional bifurcation diagram for the case  $\alpha_j = 0$  as a function of the forward and reverse bias in the gain and absorber sections  $J_1$  and  $J_2$ . Finding the region of stability in Fig. 2a) required 24 hours on a standard PC using the FM, instead of several months integrating the full DAE system. Figure 2 (b) depicts the spatio-temporal LB profile obtained with the FM method.

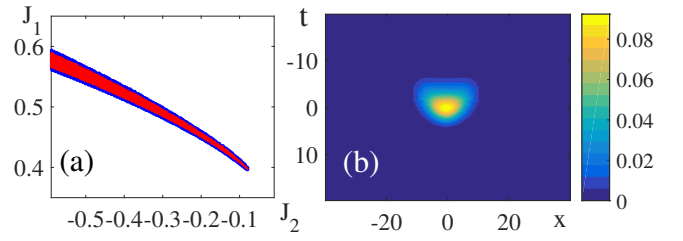


Figure 2. (a) Two-dimensional bifurcation diagram showing the region of stable existence of the LBs of the DAE model (5-7) as a function of the reverse bias in the gain and absorber sections  $J_1$  and  $J_2$ . (b) Spatio-temporal profile of the field found with the FM with  $(J_1, J_2) = (0.498, -0.336)$ . Other parameters are  $(\alpha_1, \alpha_2, h, \gamma_1, \gamma_2, s, \eta) = (0, 0, 2, 0.003, 0.1, 30, 0.5)$ .

#### ACKNOWLEDGEMENTS

C.S. and J.J. acknowledge the financial support of the MINECO Project MOVELIGHT (PGC2018-099637-B-I00 AEI/FEDER UE). S.G. acknowledges the PRIME program of the German Academic Exchange Service (DAAD) with funds from the German Federal Ministry of Education and Research (BMBF).

#### REFERENCES

- [1] U. Keller and A. C. Tropper. Passively modelocked surface-emitting semiconductor lasers. *Physics Reports*, 429(2):67 – 120, 2006.
- [2] N. Takeuchi, N. Sugimoto, H. Baba, and K. Sakurai. Random modulation cw lidar. *Appl. Opt.*, 22(9):1382–1386, May 1983.
- [3] E. Avrutin and J. Javaloyes. *Mode-Locked Semiconductor Lasers, Book Chapter In: Handbook of Optoelectronic Device Modeling and Simulation*. CRC press, Taylor and Francis, United Kingdom, 2017.
- [4] H. A. Haus. Mode-locking of lasers. *IEEE J. Selected Topics Quantum Electron.*, 6:1173–1185, 2000.
- [5] A. G. Vladimirov and D. Turaev. Model for passive mode locking in semiconductor lasers. *Phys. Rev. A*, 72:033808, Sep 2005.
- [6] J. Mulet and S. Balle. Mode locking dynamics in electrically-driven vertical-external-cavity surface-emitting lasers. *Quantum Electronics, IEEE Journal of*, 41(9):1148–1156, 2005.
- [7] Mikkel Heuck, Søren Blaaberg, and Jesper Mørk. Theory of passively mode-locked photonic crystal semiconductor lasers. *Opt. Express*, 18(17):18003–18014, Aug 2010.
- [8] Lina Jaurigue, Oleg Nikiforov, Eckehard Schöll, Stefan Breuer, and Kathy Lüdge. Dynamics of a passively mode-locked semiconductor laser subject to dual-cavity optical feedback. *Phys. Rev. E*, 93:022205, Feb 2016.
- [9] R. M. Arhipov, T. Habruseva, A. Pimenov, M. Radziunas, S. P. Hegarty, G. Huyet, and A. G. Vladimirov. Semiconductor mode-locked lasers with coherent dual-mode optical injection: simulations, analysis, and experiment. *J. Opt. Soc. Am. B*, 33(3):351–359, Mar 2016.
- [10] M. Marconi, J. Javaloyes, S. Balle, and M. Giudici. Passive mode-locking and tilted waves in broad-area vertical-cavity surface-emitting lasers. *Selected Topics in Quantum Electronics, IEEE Journal of*, 21(1):85–93, Jan 2015.
- [11] M. Marconi, J. Javaloyes, S. Balle, and M. Giudici. How lasing localized structures evolve out of passive mode locking. *Phys. Rev. Lett.*, 112:223901, Jun 2014.
- [12] C. Schelte, J. Javaloyes, and S. V. Gurevich. Functional mapping for passively mode-locked semiconductor lasers. *Opt. Lett.*, 43(11):2535–2538, Jun 2018.
- [13] J. Javaloyes. Cavity light bullets in passively mode-locked semiconductor lasers. *Phys. Rev. Lett.*, 116:043901, Jan 2016.
- [14] S. V. Gurevich and J. Javaloyes. Spatial instabilities of light bullets in passively-mode-locked lasers. *Phys. Rev. A*, 96:023821, Aug 2017.